Physics in Medicine & Biology

IPEM Institute of Physics and Engineering in Medicine

PAPER • OPEN ACCESS

Investigating the impact of the effective point of measurement for plane-parallel ionization chambers in clinical proton beams

To cite this article: Kilian-Simon Baumann *et al* 2025 *Phys. Med. Biol.* **70** 015014

IOP Publishing Phys. Med. Biol. 70 (2025) 015014 https://doi.org/10.1088/1361-6560/ad9e7c

Physics in Medicine & Biology

IPEM Institute of Physics and Engineering in Medicine

OPEN ACCESS

RECEIVED
16 August 2024

REVISED
28 November 2024

ACCEPTED FOR PUBLICATION
12 December 2024

PUBLISHED
27 December 2024

PAPER

Investigating the impact of the effective point of measurement for plane-parallel ionization chambers in clinical proton beams

Kilian-Simon Baumann[1,2,3,4,*], **Ana Lourenço**[5,6], **Jörg Wulff**[7,8], **Gloria Vilches-Freixas**[9] and **Hugo Palmans**[5,10]

[1] Department of Radiotherapy and Radiooncology, University Medical Center Giessen-Marburg, Marburg, Germany
[2] University of Applied Sciences, Institute of Medical Physics and Radiation Protection, Giessen, Germany
[3] Marburg Ion-Beam Therapy Center (MIT), Marburg, Germany
[4] LOEWE Research Cluster for Advanced Medical Physics in Imaging and Therapy (ADMIT), TH Mittelhessen University of Applied Sciences, Giessen, Germany
[5] National Physical Laboratory, Teddington, United Kingdom
[6] University College London, London, United Kingdom
[7] West German Proton Therapy Centre Essen WPE, Essen, Germany
[8] University Hospital Essen, West German Cancer Center WTZ, Essen, Germany
[9] Department of Radiation Oncology (Maastro), GROW Research Institute for Oncology and Reproduction, Maastricht University Medical Centre, Maastricht, The Netherlands
[10] MedAustron Ion Therapy Center, Wiener Neustadt, Austria
[*] Author to whom any correspondence should be addressed.

E-mail: kilian-simon.baumann@staff.uni-marburg.de

Keywords: proton reference dosimetry, proton therapy, effective point of measurement, response functions, Monte Carlo, GEANT4

Abstract

Objective. To investigate the impact of the positioning of plane-parallel ionization chambers in proton beams on the calculation of the chamber-specific factor f_Q and, hence, the beam quality correction factor k_{Q,Q_0}. *Approach.* Monte Carlo simulations were performed to calculate the chamber-specific factor f_Q in monoenergetic proton beams for six different plane-parallel ionization chambers while positioning the chambers with a) their reference point and b) their effective point of measurement accounting for the water equivalent thickness of the entrance window. *Main results.* For all ionization chamber models investigated in this study, the difference in f_Q between both positioning approaches was larger for steeper dose gradients and bigger differences between the geometrical thickness and water-equivalent thickness of the entrance window. The largest effect was 1.2% for the IBA PPC-05 ionization chamber at an energy of 60 MeV. *Significance.* The positioning of plane-parallel ionization chambers in proton beams has a systematic impact on the f_Q factor. This is especially of relevance for the k_{Q,Q_0} factors presented in the recently updated TRS-398 code of practice (CoP) from IAEA. The background is that a positioning with the effective point of measurement is prescribed in TRS-398 CoP, however, all Monte Carlo derived data that have been employed for the update are based on a positioning of the ionization chambers with their reference point. Hence, the updated k_{Q,Q_0} factors for plane-parallel ionization chambers in proton beams are subject to systematic errors that can be as large as 0.5%.

1. Introduction

For the determination of absorbed dose-to-water with air-filled ionization chambers, dosimetry protocols such as the TRS-398 code of practice (CoP) published by the IAEA are typically used in the clinical routine. The first version of the TRS-398 CoP was published in 2000 IAEA (2000) and updated in 2024 (TRS-398 CoP, Rev. 1) IAEA (2024). The TRS-398 CoP defines the exact reference conditions including measurement depth, positioning of the ionization chamber and which ionization chamber type should be used for a certain beam quality. For pencil beam scanning proton beams, in the updated version, TRS-398 CoP, Rev. 1, both, cylindrical and plane-parallel ionization chambers are recommended for proton beams with the limitation that cylindrical ionization chambers should only be used in single pencil beams with residual ranges (R_{res})

larger than 15 g cm^{-2} Palmans *et al* (2020, 2022). The background is that the dose gradient at the measurement depth is known to impact the reading of cylindrical ionization chambers due to the effective point of measurement (P_{eff}), approximated at 0.75 times the inner cavity radius closer to the beam source for protons Palmans *et al* (2020)[11]. TRS-398 CoP prescribes a positioning of cylindrical ionization chambers with their reference point (P_{ref}) at the measurement depth which is located at the center of the central electrode. Given P_{eff}, the positioning of the reference point only leads to accurate results if the ionization chamber is used in conditions with negligible dose gradients which is the case for $R_{\text{res}} \geqslant 15$ g cm^{-2}.

For plane-parallel ionization chambers, TRS-398 CoP, Rev. 1 also prescribes the positioning of the ionization chamber with P_{ref} at the measurement depth which is 2 g cm^{-2} for $R_{\text{res}} \geqslant 5$ g cm^{-2} and 1 g cm^{-2} for $R_{\text{res}} < 5$ g cm^{-2} in pencil beam scanning proton beams (see table 36 in TRS-398 CoP, Rev. 1). P_{ref} is defined at the center of the inner surface of the entrance window. However, in chapter 4.2.5.2 it is instructed to account for the water-equivalent thickness (WET) of the entrance window when positioning the ionization chamber in charged particle beams and thus to consider an effective point of measurement, P_{eff}, that is different from P_{ref}. This is also depicted in figure 21 in part b in TRS-398 CoP, Rev. 1 where the thickness of the entrance window t_{wall} is defined as the WET. Despite some possible ambiguity in the tables and figures in TRS-398 CoP, Rev. 1, it generally assumes the consideration of P_{eff} in reference dosimetry with plane-parallel ionization chambers Private communication with Stanislav Vatnitsky (2024).

The concept of WET is well understood for proton beams and can be easily parametrized Zhang and Newhauser (2009), Zhang *et al* (2010), Lourenco *et al* (2016). The WET of the entrance window accounts for a stopping power and the corresponding energy loss in material different than that of water. As a result, P_{eff} can be located at a different depth compared to P_{ref} as shown in figure 1. In this approximation, P_{eff} only accounts for the WET of the entrance window and not for any other possible perturbation effects. If the ratio of the WET and the physical thickness is larger than unity (e.g. for materials with a stopping power larger than that of water) P_{eff} is located at a larger depth compared to P_{ref}. If the ratio of the WET and the physical thickness is smaller than unity it is the other way round and P_{eff} is located at a shallower depth compared to P_{ref}. The latter occurs for the ionization chambers Markus and Advanced Markus from the manufacturer PTW (Physikalisch Technische Werkstätten, Freiburg, Germany) that have a layer of air inside the entrance window. In the case that a dose gradient is present at the measurement depth, this effect has to be accounted for since different doses will be determined if P_{ref} or P_{eff} is positioned at the reference depth.

During the update of the TRS-398 CoP, the RTNORM project RTNORM (2019) provided data for beam-quality correction factors k_{Q,Q_0} in clinical proton beams. Next to the experimental determination of k_{Q,Q_0} factors using calorimetry, several Monte Carlo based studies were published that calculated chamber-specific factors f_Q, perturbation correction factors p, and k_{Q,Q_0} factors for air-filled ionization chambers Gomà *et al* (2016), Wulff *et al* (2018), Goma Sterpin (2019), Kretschmer *et al* (2020), Baumann *et al* (2020a, 2020b, 2021). The results from these studies were then used by Palmans *et al* (2022) to derive best estimates of beam-quality correction factors k_{Q,Q_0} for proton beams that have been incorporated in TRS-398 CoP, Rev. 1. Best estimates of k_{Q,Q_0} for plane-parallel ionization chambers were based on the average overall perturbation correction factor $\langle p_Q \rangle$ for each ionization chamber model individually from published data. Average $\langle f_Q \rangle$ and corresponding k_{Q,Q_0} factors were calculated as:

$$\langle f_Q \rangle = \langle p_Q \rangle \cdot s_{\text{w,air}} \tag{1}$$

$$k_{Q,Q_0} = \frac{\langle f_Q \rangle \cdot (W_{\text{air}})_Q}{f_{Q_0} \cdot (W_{\text{air}})_{Q_0}} \tag{2}$$

with $s_{\text{w,air}}$ being the stopping-power ratio water-to-air of protons and W_{air} being the mean energy needed to create and electron-ion-pair in air depending on the beam qualities Q and Q_0.

In the determination of k_{Q,Q_0} according to equation (2), it was assumed that no displacement correction was necessary for plane-parallel ionization chambers in proton beams, e.g. $p_{\text{dis}} = 1$. This is motivated by the fact that in TRS-398 CoP it is considered that plane-parallel ionization chambers are positioned with P_{eff} at the measurement depth (see above). However, in all Monte-Carlo based studies used for the data analysis performed by Palmans *et al* (2022), the ionization chambers have been positioned with P_{ref} at the measurement depth without accounting for the WET of the entrance windows. According to figure 1, this leads to a displacement correction factor $p_{\text{dis}} \neq 1$, if 1) the WET of the entrance window is differing from its geometrical thickness and 2) a significant dose gradient is present at the measurement depth. As a direct consequence of the inconsistency between the positioning approach specified in the TRS-398 CoP and the

[11] Note that this factor of 0.75 times the inner cavity radius employed for protons is similar to the factor recommended for light ions.

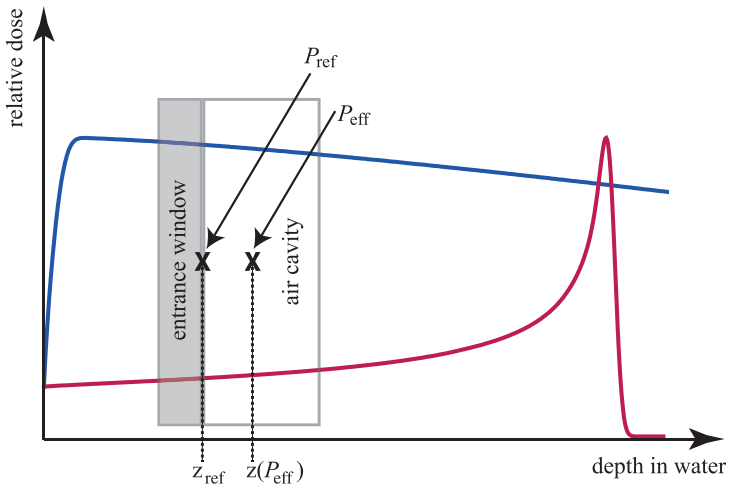

Figure 1. Schematic influence of the effective point of measurement (P_{eff}): Depicted are qualitative depth-dose distributions for ^{60}Co radiation (blue) and protons (red). The simplified cross-section of a plane-parallel ionization chamber is shown with the reference point (P_{ref}) and P_{eff}. Note that for ionization chambers where the WET of the entrance window is smaller than the geometrical thickness, P_{eff} is located at a shallower depth compared to P_{ref} (at is is the case for the PTW Markus and Adv. Markus chamber). In the case of protons, the absorbed dose-to-water (D_w) at the depth of P_{eff} ($z(P_{eff})$) is larger compared to the dose at the depth of P_{ref} (z_{ref}) and, hence, the factor f_Q is larger when accounting for P_{eff}. For ^{60}Co radiation, it is the other way round. Note that the positioning depth of ionization chambers is different in proton beams compared to ^{60}Co radiation but was chosen to be the same in this scheme for the sake of simplicity. The chamber geometry is not depicted true to scale. Please note that the scenario depicted here (P_{ref} located at the reference depth) was used for the Monte Carlo simulations within the RTNORM project to provide k_{Q,Q_0} factors whereas the TRS-398 CoP, Rev. 1 defines a positioning of P_{eff} at the measurement depth.

one used in the Monte-Carlo studies, k_{Q,Q_0} factors published by Palmans *et al* (2022) and presented in the updated version of the TRS-398 CoP might be subject to systematic errors Vilches-Freixas *et al* (2024).

These errors will strongly depend on the ionization chamber geometry, e.g. the WET of the entrance window, and the energy of the protons defining the dose gradient at the measurement depth. Hence, the goals of this study are:

- To determine the WET of different plane-parallel ionization chambers and hence the resulting shift between P_{ref} and P_{eff}
- To demonstrate that the impact of P_{eff} is dominated by the dose gradient at the measurement depth and the WET of the entrance window
- To re-calculate the chamber-specific factor f_Q of plane-parallel ionization chambers while accounting for the WET of the entrance windows and quantify the impact of both positioning approaches (P_{ref} versus P_{eff})
- To re-analyze the best estimate of k_{Q,Q_0} factors according to the approach employed by Palmans *et al* (2022)
- To provide an upper limit of the systematic error of k_{Q,Q_0} factors published in the TRS-398 CoP, Rev. 1 resulting from the positioning inconsistency

2. Materials and methods

2.1. Monte Carlo calculation of f_Q factors

The chamber-specific factor f_Q of ionization chambers is the basis of beam quality correction factors k_{Q,Q_0} which can be calculated as follows Andreo *et al* (2013):

$$k_{Q,Q_0} = \frac{f_Q}{f_{Q_0}} \frac{W_{air,Q}}{W_{air,Q_0}} = \frac{(D_w/\bar{D}_{air})_Q}{(D_w/\bar{D}_{air})_{Q_0}} \frac{W_{air,Q}}{W_{air,Q_0}} \quad (3)$$

Q denotes the user beam quality and Q_0 the reference beam quality. The chamber-specific factor f is both chamber-specific and beam quality-dependent and gives the proportionality between the absorbed dose-to-water at the measurement depth when the chamber is absent (D_w) and the average absorbed dose-to-air in the active cavity of the air-filled ionization chamber ($\bar{D}_{air}$) Sempau *et al* (2004). $W_{air,Q}$ is the mean energy necessary to create an ion pair in air.

In this study, we focus on the Monte Carlo calculation of f_Q for plane-parallel ionization chambers in clinical proton beams for different positioning approaches. The dose values D_w were calculated using the

Monte Carlo code TOPAS version 3.7 based on GEANT4 version geant4-10-06-patch-03. D_w was calculated in a disk of water with a thickness of 250 μm and a diameter of 10 mm placed in a water phantom of $20 \times 20 \times 5$ cm^3. $\bar{D}_{air}$ was not calculated specifically in this study but values for $\bar{D}_{air}$ were taken from Baumann *et al* (2023) who used the same version of TOPAS. In that study, ionization chambers were positioned with P_{ref} at the measurement depth which is 1 g cm^{-2} for low energies (60 and 70 MeV) and 2 g cm^{-2} for higher energies (80, 100, 150, 160, 200 and 250 MeV). Note that the unit g cm^{-2} does not mean that the authors accounted for the WET of the entrance window when positioning the ionization chamber but only for the mass density of water of 0.9982 g cm^{-3} Seltzer *et al* (2016). Geometrical depths of 1.0018 cm and 2.0036 cm resulted accordingly.

To investigate the influence of the positioning approaches the position of the water voxel which is used to calculate D_w was altered instead of shifting the ionization chamber models: for the positioning of the ionization chamber with P_{ref}, the water voxel was placed with its center at the measurement depths of 1 g cm^{-3} and 2 g cm^{-3}, respectively, which is the same depth as the reference point of the ionization chamber. To account for P_{eff}, the position of the water voxel was shifted corresponding to the shift between P_{eff} and P_{ref}, whereas this shift was determined for each ionization chamber individually as described in section 2.3. The factor f_Q was calculated from the two sets of D_w and $\bar{D}_{air}$ values.

The approach of shifting the water voxel rather than the ionization chambers was chosen to save computing time since the absorbed doses-to-water can be calculated simultaneously for all ionization chambers within one simulation for each energy instead of setting up a simulation for all ionization chambers and energies individually. The distance between the source and water phantom is kept constant for all simulations, only the position of the water voxel within the phantom is shifted accordingly. To demonstrate that this approach is justified the change in f_Q by shifting the ionization chamber instead of the water voxel was calculated for one ionization chamber. The difference in f_Q between shifting the water voxel and shifting the ionization chamber was in the order of 0.1% which is comparable to the type-A uncertainty.

2.2. Ionization chamber characteristics

Six plane-parallel ionization chambers (PTW Roos, PTW Markus, PTW Advanced Markus, IBA NACP-02, IBA PPC-05 and IBA PPC-40) were investigated. The exact same chamber geometries and material compositions were taken as used in previous studies by Baumann *et al* (2020a, 2020b, 2021) obtained from manufacturer's blue prints and employing the latest values from ICRU 90 report Seltzer *et al* (2016) for mass densities and mean excitation potentials. The design specifications of the entrance windows are summarized in table 1. For each material of the entrance window, the geometrical thickness and mass density is provided as well as the areal mass density as the product of geometrical thickness times mass density.

2.3. Determination of the effective point of measurement as a results of entrance chamber's WET (P_{eff})

The position of P_{eff} due to the WET of the ionization chamber's entrance window was calculated for each ionization chamber model. The depth-dose curve of an 80 MeV proton beam in water was calculated with Monte Carlo with a resolution of 0.1 mm. For each ionization chamber, the entrance window was then placed in front of the water volume and the corresponding depth-dose distribution was scored. The shift between both curves corresponds to the WET of the entrance window and was determined as minimized squared differences with:

$$\mathrm{WET} = \min_s \sum_z \left(d_0(z) - d(z+s)\right)^2 \tag{4}$$

where $d_0(z)$ is the reference curve as a function of depth z and $d(z+s)$ is the depth dose distribution with the entrance window in the beam shifted by s.

By subtracting the geometrical thickness of the entrance window from the WET, the shift of P_{eff} relative to P_{ref} can be determined. If the WET of an entrance window is larger than the geometrical one this shift is positive and means that P_{eff} is located at a larger depth compared to P_{ref} and, hence, is located inside the air-filled cavity. If it is the other way round P_{eff} is located at a shallower depth compared to P_{ref} and is located inside the entrance window. Note that P_{eff} as used in this study only accounts for the WET of the entrance window and not any other fluence perturbations that might be introduced by the materials deployed in the ionization chamber geometry.

The WET slightly depends on proton energy since the stopping-power ratio is not constant. Hence, we also determined the WET of the entrances windows at a proton energy of 250 MeV.

Additionally, we calculated the WET of each entrance window following the approach by Zhang and Newhauser (2009) at an energy of 80 MeV by calculating ratios of stopping powers between the materials employed and water.

2.4. Calculation of dose gradients

In addition to the calculation of f_Q with and without consideration of P_{eff}, the dose gradient of the absorbed dose-to-water at the measurement depth was calculated for monoenergetic proton beams of the same energies as used for the calculation of f_Q. The laterally integrated depth dose distributions were scored with a resolution of 0.01 mm in depth and a lateral dimension of 10×10 cm^2. The depth dose distribution was linearly interpolated between each two grid points. The dose gradient was calculated as the difference in absorbed dose-to-water at the depths of P_{ref} and P_{eff} divided by the shift between both depths.

2.5. Depth dependence of p_Q for the IBA PPC-05 ionization chamber

To investigate the role of P_{eff} for relative dosimetry, the effect of P_{eff} on the measurement of a depth-dose distribution was investigated. The laterally integrated depth-dose distribution of 200 MeV protons in water was calculated. Subsequently, the absorbed dose-to-water in the air cavity of the IBA PPC-05 ionization chamber was simulated whereas the ionization chamber was positioned at different depths in water. For each depth, the two positioning approaches were investigated.

Additionally, the f_Q factor was calculated for each depth and the two positioning approaches. From f_Q factors, the overall perturbation correction factor p_Q was calculated by dividing f_Q by the mass stopping-power ratio water-to-air ($s_{\text{w,air}}$) calculated as a function of residual range following TRS-398 CoP, Rev. 1.

2.6. Settings for Monte Carlo simulations with TOPAS

For all Monte Carlo simulations, the Monte Carlo code GEANT4 Agostinelli *et al* (2003) version geant4-10-06-patch-03 was used in combination with the toolkit TOPAS Perl *et al* (2012) version 3.7. In this study, the same physics lists and transport parameters were applied as used by Baumann *et al* (2020a, 2020b, 2023). In short:

- The physics modules *g4em-standard_opt4*, *g4h-phy_QGSP_BIC_HP*, *g4ion-binarycascade*, *g4decay*, *g4h-elastic_HP* and *g4stopping* were employed
- *dRoverR*, the parameter controlling the length of a condensed-history step, was set to 0.05
- Particles were transported down to a residual range of 100 nm
- The production cut in the water phantom was set to 500 μm, corresponding to ~200 keV electrons in water
- Within the ionization chamber geometry and a surrounding envelope, the production cut-off was set to 1 μm, corresponding to <10 keV electrons in water
- This envelope was designed to be larger than the ionization chamber geometry by 500 μm (production cut applied in the water phantom) multiplied by a safety margin of 1.2 to avoid a disturbance of the particle fluence within the ionization chamber geometry by the larger production threshold applied in the water phantom

No variance reduction techniques were used. The statistical uncertainties were estimated by combining the uncertainties from independent runs performed with different random seeds as described by Bielajew (2016).

2.7. Impact of simplified field configurations in Monte Carlo simulations

In the Monte Carlo simulations performed in this study, the proton beam was simplified by using a homogeneous 10×10 cm^2 field impinging perpendicular on the water phantom surface using monoenergetic protons. In clinical settings, the beam is neither monoenergetic nor are the individual pencil beams perfectly parallel to each other if the active scanning application technique is employed.

The possible impact of the simplifications was investigated for the IBA PPC-05 ionization chamber at 60 MeV where the largest effect of P_{eff} was observed. The change in f_Q due to P_{eff} was calculated for 1) various energy spreads and 2) scanned proton fields. For the energy spread, a normally distributed energy distribution of the particles was assumed and the width of this distribution in terms of σ was chosen to be 0.3%, 1% and 10% of the nominal energy (in this case 60 MeV). The energy spread of 10% was used as an extreme upwards estimation which is technically not feasible in clinical accelerators. For the scanned fields, two different distances of 1 m and 7 m between the center of the virtual scanning magnets and the iso-center were investigated. As source, a pencil beam with a full width at half maximum (FWHM) of 26.3 mm was employed. The beam was deflected at the position of the center of the scanning magnets to scan a homogeneous field of 10×10 cm^2 at the iso-center with a lateral spot spacing of 2 mm. The front of the water phantom was placed in the iso-center and D_{w} and $\bar{D}_{\text{air}}$ were calculated as described in section 2.1.

2.8. Experimental determination of the impact of P_{eff}

To demonstrate that the impact of P_{eff} is dominated by the dose gradient, experiments were performed at Marburg Ion-Beam Therapy Center Zink *et al* (2024) and Maastro Proton Therapy Center Vilches-Freixas

et al (2020). At Marburg Ion-Beam Therapy Center, the PTW Advanced Markus ionization chamber was used to measure the collected charge in a 10×10 cm^2 homogeneous proton field. A 3 mm spot spacing was used with beam widths between 8.1 mm and 20.3 mm (full-width half maximum in air at the isocenter) depending on proton energy. Measurements were performed at energies of 78.10, 113.33, 153.89, 198.13 and 220.65 MeV/u. Experiments with the IBA PPC-05 chamber were performed at the Maastro Proton Therapy Center. Again, charge was collected in a 10×10 cm^2 homogeneous proton field with a spot spacing of 2.5 mm and beam widths between 9.7 and 32.0 mm (full-width half maximum in air at the isocenter) depending on the proton energy. Measurements were performed for proton energies of 78.2, 113.1, 153.9, 198.1 and 227 MeV.

At both centers, the ionization chambers were positioned within a water phantom at a measurement depth of 20 mm at the center of the irradiated proton field, i.e. reference depth according to TRS-398 CoP, Rev. 1. Measurements were taken with the two positioning approaches (P_{ref} and P_{eff}) for each energy. The ionization chamber reading was corrected for air pressure and temperature. Subsequently, the difference in collected charge for both positioning approaches was compared to the corresponding dose gradient at the measurement depth. The dose gradient at the measurement depth was extracted from previously acquired depth-dose curves.

Additionally, another set of measurements was acquired for each energy at a depth chosen in the proximal rise of the pristine Bragg peak for each energy in order to validate the impact of P_{eff} for a larger variety of dose gradients. The measurement depths are shown in tables 3 and 4.

3. Results and discussion

3.1. Ionization chamber characteristics

Table 1 shows the dimensions and materials of the entrance windows of the plane-parallel ionization chambers investigated in this study. Additionally, the stopping power ratio (SPR) of each material in relation to water is given for 80 MeV protons calculated according to Zhang and Newhauser (2009). Furthermore, areal mass density, geometrical thickness, Monte-Carlo derived WET (for 80 and 250 MeV protons) and the shift between P_{ref} and P_{eff} are displayed. As expected, for all ionization chamber models, there is a difference between the geometrical thickness and WET of the entrance window resulting in an effective shift of P_{eff} relative to P_{ref}. For the PTW Markus and Adv. Markus chamber, this shift is negative, since the entrance window contains air with a small WET leading to a larger geometrical thickness compared to the WET[12]. For all other ionization chambers, the shift is positive meaning that the WET is larger than the geometrical thickness. The maximum shift is 0.59 mm for the IBA PPC-05 ionization chamber. For all ionization chambers, the WET agrees within 0.6 mm or better between 80 MeV and 250 MeV.

The areal mass agrees with the WET within 2.6% (corresponding to $\leqslant 0.03$ mm) or better for all ionization chambers except for the IBA NACP-02 and PPC-05. The background is that for the materials employed in the entrance windows of these two ionization chambers, the SPR is significantly different than unity. According to TRS-398 CoP, Rev. 1, the WET can be approximated by the areal mass for plastics not thicker than 5 mm which is the case for all ionization chambers investigated in this study. For the PTW ionization chambers and the PPC-40, the areal mass is larger than the WET for 80 MeV protons and smaller than the WET for 250 MeV protons. For the PPC-05 and NACP-02, the areal mass is larger than the WET by up to 0.19 mm.

Another possibility of calculating the WET is based on SPR Zhang and Newhauser (2009). When doing so, the difference between Monte Carlo derived WET and WET based on SPR is 0.03 mm at maximum for 80 MeV protons and the PPC-05 chamber. For all residual chambers the difference is 0.01 mm at maximum.

3.2. Influence of effective point of measurement on simulation of f_Q factors

In figure 2, f_Q factors as a function of proton energy are shown for the six plane-parallel ionization chambers investigated in this study with and without accounting for P_{eff}. The general behavior of f_Q factors will not be discussed here as it has been done in previous studies Gomà *et al* (2016), Wulff *et al* (2018), Goma Sterpin (2019), Kretschmer *et al* (2020), Baumann *et al* (2020a, 2021, 2023). When accounting for P_{eff}, f_Q is smaller for the PTW Markus and Adv. Markus chamber and larger for all other investigated chambers. This behavior between the ionization chamber models agrees with the shift of P_{eff} relative to P_{ref} as shown in table 1 which is negative for the PTW Markus and Adv. Markus chamber and positive for all other chambers. The difference in f_Q factors between both positioning approaches is larger for low proton energies and decreases with increasing energy. For energies of 150 MeV or higher, the difference is generally smaller than 0.3% for

[12] The difference in WET for 250 MeV between PTW Markus and Adv. Markus is smaller than the resolution of the depth dose distribution used for deriving the WET and hence not significant. Both chamber types have the same design of the entrance window.

Table 1. Dimensions and materials of the entrance windows of the plane-parallel ionization chambers based on manufacturer's specifications. The mass density of each material is given in brackets. The abbreviations used are: PET for Polyethylene terephthalate, PMMA for Polyether methacrylate, and PE for Polyethylene. Additionally, the stopping power ratio (SPR) of each material in relation to water is given for 80 MeV protons calculated according to Zhang and Newhauser (2009). Furthermore, the areal mass in g cm^{-2}, the geometrical thickness in mm, the WET in mm and the shift between P_{ref} and P_{eff} is given, as well. The values for WET were calculated based on SPR as well as Monte Carlo simulations. The shift of P_{eff} relative to P_{ref} is based on Monte Carlo derived WET.

Ionization chamber	Design of entrance window	SPR material to water	Areal mass density in g cm^{-2}	Geometrical thickness in mm	WET in mm via SPR Zhang and Newhauser (2009) for 80 MeV	Monte Carlo derived WET in mm for 80 MeV	Monte Carlo derived WET in mm for 250 MeV	Shift of P_{eff} relative to P_{ref} in mm for 80 MeV	Shift of P_{eff} relative to P_{ref} in mm for 250 MeV
PTW									
Roos	1.1 mm PMMA (1.19 g cm^{-3}) 20 μm graphite (0.82 g cm^{-3})	1.165 0.734	0.133	1.120	1.30	1.30	1.36	0.18	0.24
Markus	0.87 mm PMMA (1.19 g cm^{-3}) 0.4 mm Air (1.20 mg cm^{-3}) 30 μm PE (0.93 g cm^{-3})	1.165 0.001 0.997	0.106	1.300	1.04	1.05	1.08	−0.25	−0.22
Advanced Markus	0.87 mm PMMA (1.19 g cm^{-3}) 0.4 mm Air (1.20 mg cm^{-3}) 30 μm PE (0.93 g cm^{-3})	1.165 0.001 0.997	0.106	1.300	1.04	1.05	1.07	−0.25	−0.23
IBA									
NACP-02	0.1 mm PET/Mylar (1.4 g cm^{-3}) 0.5 mm grahpite (1.82 g cm^{-3})	1.311 1.630	0.105	0.600	0.95	0.95	0.98	0.35	0.38
PPC-05	0.95 mm C552 (1.76 g cm^{-3}) 50 μm graphite (1.82 g cm^{-3})	1.601 1.630	0.176	1.000	1.60	1.57	1.59	0.57	0.59
PPC-40	0.9 mm PMMA (1.19 g cm^{-3}) 0.1 mm graphite (0.93 g cm^{-3})	1.165 0.833	0.116	1.000	1.13	1.13	1.18	0.13	0.18

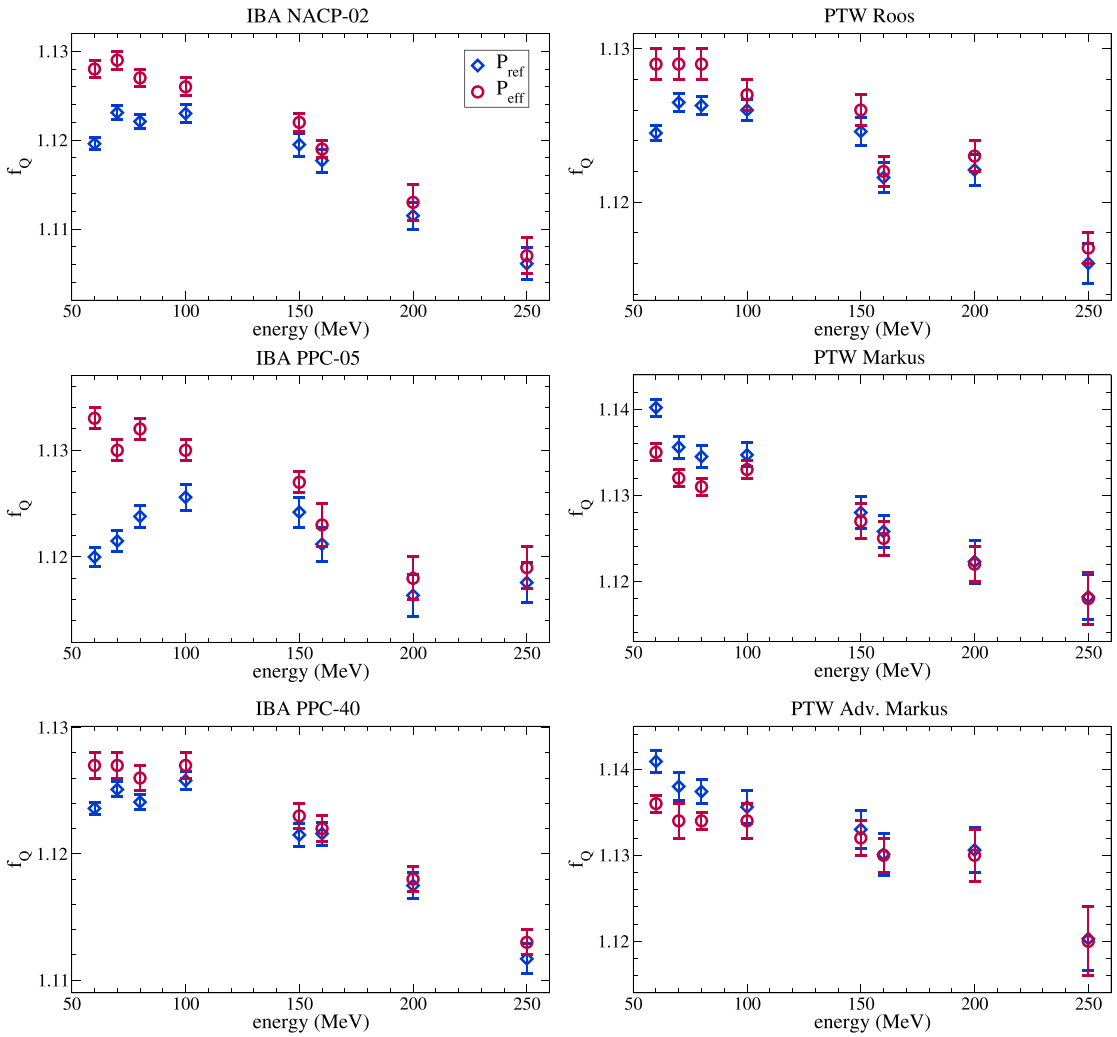

Figure 2. Monte Carlo calculated f_Q factors for monoenergetic proton beams as a function of initial proton energy for different plane-parallel ionization chambers with and without accounting for P_{eff}. The error bars correspond to one standard uncertainty.

all ionization chambers investigated. The largest effect of 1.2% can be observed for the IBA PPC-05 ionization chamber at an energy of 60 MeV. In general, the larger the shift between P_{ref} and P_{eff}, the larger the difference between f_Q factors. When accounting for P_{eff}, the dependence of f_Q on proton energy seems to be less pronounced for low energies of up to 100 MeV for some ionization chambers. For example, f_Q factors for the IBA PPC-05 ionization chamber vary by 0.5% between 60 MeV and 100 MeV when positioning the chamber with P_{ref} but this variation decreases to 0.3% when accounting for P_{eff}.

3.3. Impact of dose gradient

Table 2 summarizes the difference in D_w as well as f_Q for both positioning approaches. The change in D_w between both positioning approaches was derived from the dose gradient at the measurement depth whereas the change in f_Q was explicitly calculated as described in section 2.1. The difference between the change in D_w and the change in f_Q is smaller than 0.1% for all ionization chambers. This indicates that the change in f_Q is a result of the dose gradient at the measurement depth. This was found for all ionization chambers and proton energies investigated in this study.

The results of the experimental investigation are summarized in tables 3 and 4. The differences in collected charge with a PTW Advanced Markus and IBA PPC-05 ionization chamber are shown for different proton energies at different measurement depths. For each measurement depth, both positioning approaches have been used. Additionally, the dose difference at the corresponding measurement depths and proton energies are shown that were extracted from previously measured depth-dose curves. The uncertainty of this dose difference was estimated by a positioning uncertainty of 0.1 mm. Note that, in contrast to the difference in f_Q, the difference in collected charge for the PTW Advanced Markus ionization chamber is positive. The reason is that P_{eff} is located at a shallower depth compared to P_{ref} leading to a positioning of the ionization chamber at a larger depth when employing P_{eff}. The differences in collected charge between both positioning

Table 2. The difference in absorbed dose-to-water (D_w) between the depths of P_{ref} and P_{eff} for 60 MeV protons compared to the change in f_Q due to P_{eff}.

Ionization chamber model	$\Delta D_w(P_{eff} - P_{ref})$ in %	$\Delta f_Q(P_{eff} - P_{ref})$ in %
PTW Roos	0.37	0.38
PTW Markus	−0.49	−0.46
PTW Adv. Markus	−0.50	−0.47
IBA NACP-02	0.74	0.75
IBA PPC-05	1.17	1.19
IBA PPC-40	0.30	0.28

Table 3. Differences in measured charge C between positioning of the ionization chamber with P_{ref} and P_{eff} at the measurement depth for the PTW Advanced Markus ionization chamber in scanned proton beams of different energies at different measurement depths. Additionally, the corresponding difference in dose D extracted from depth-dose curves in given. The uncertainty due to the positioning of the chamber is given in brackets. Note that the differences are positive since P_{eff} is located at a shallower depth compared to P_{ref}.

Proton energy in MeV	Measurement depth in mm	$\Delta C(P_{eff} - P_{ref})$ in %	$\Delta D(P_{eff} - P_{ref})$ in %
78.10	20	0.3	0.4(1)
	40.2	1.5	1.7(5)
113.33	20	0.3	0.2(1)
	85.5	1.0	1.2(5)
153.89	20	0.0	0.1(1)
	153.2	0.9	1.0(4)
198.13	20	0.0	0.1(1)
	243.7	0.9	0.9(3)
220.65	20	0.1	0.1(1)
	289.7	0.3	0.6(2)

Table 4. Differences in measured charge C between positioning of the ionization chamber with P_{ref} and P_{eff} at the measurement depth for the IBA PPC-05 ionization chamber in scanned proton beams of different energies at different measurement depths. Additionally, the corresponding difference in dose D extracted from depth-dose curves in given. The uncertainty due to the positioning of the chamber is given in brackets. Note that the differences are negative since P_{eff} is located deeper compared to P_{ref}.

Proton energy in MeV	Measurement depth in mm	$\Delta C(P_{eff} - P_{ref})$ in %	$\Delta D(P_{eff} - P_{ref})$ in %
78.2	20	−0.6	−0.8(1)
	41.5	−3.4	−3.1(5)
113.1	20	−0.4	−0.3(1)
	86.8	−3.3	−3.0(5)
153.9	20	−0.2	−0.2(1)
	153.9	−3.1	−2.9(4)
198.1	20	−0.3	−0.2(1)
	198.1	−0.5	−0.3(3)
227.0	20	−0.2	−0.2(1)
	291.0	−0.5	−0.6(2)

approaches are, in general, less pronounced for the PTW Advanced Markus ionization chamber since the shift between P_{eff} and P_{ref} is smaller. With a few exceptions, the difference in measured charge agrees within the difference in dose within the estimated uncertainty, independent on the dose gradient. The largest difference is 0.3%. Altogether, the experimental investigation demonstrates that the impact of P_{eff} is dominated by the dose gradient at the measurement depth.

3.4. Depth dependence of p_Q

In figure 3, a zoom-in to the Bragg peak region of a depth-dose curve of 200 MeV protons is shown as reference along with a point-wise simulation with the IBA PPC-05 ionization chamber with and without accounting for P_{eff}. When positioning P_{ref} at the measurement depth, i.e. not accounting for P_{eff}, the determined depth-dose distribution is shifted towards shallower depths compared to the reference curve. The shift of the depth dose distributions corresponds to the shift between P_{ref} and P_{eff} of the ionization chamber, e.g. ∼0.57 mm. If P_{eff} is considered, the determined depth-dose distribution agrees with the reference one. As a result, for measurements of depth-dose curves and especially the range of particles, P_{eff} should be accounted for when using plane-parallel ionization chambers because otherwise the range will be under- or overestimated depending on the ionization chamber used.

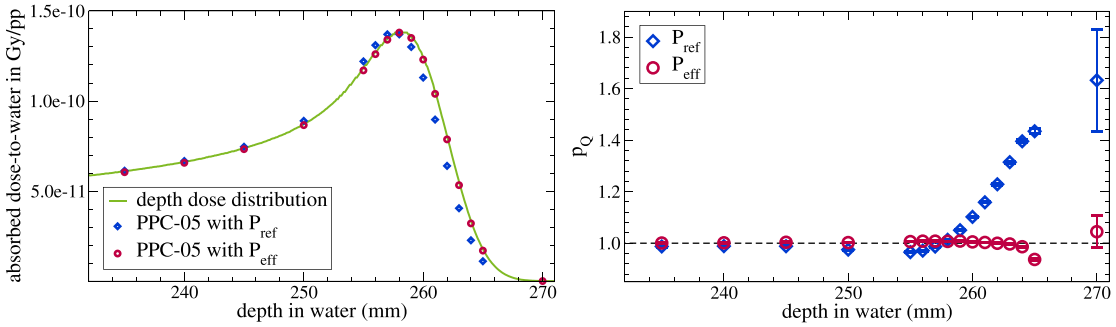

Figure 3. On the left, the depth dose distribution of 200 MeV protons is shown in a straight blue line. In red circles, the depth dose distribution is shown that is determined point-wise with an IBA-PPC-05 ionization chamber without accounting for P_{eff}. Additionally, the depth dose distribution determined with the IBA PPC-05 ionization chamber is shown when placing the chamber with P_{eff} at the measurement depth. On the right, the p_Q factor as a function of depth for an IBA PPC-05 ionization chamber at 200 MeV protons is shown with and without accounting for P_{eff}.

On the right-hand side of figure 3, the overall perturbation correction factors p_Q for the IBA PPC-05 ionization chamber are shown as a function of depth in water for 200 MeV protons, again with and without consideration of P_{eff}. When positioning the ionization chamber with P_{ref}, p_Q shows a strong dependence on depth, especially behind the Bragg peak where p_Q increases by up to ∼70%. This pronounced increase in the region of the distal fall-off is due to the shift of the depth dose distribution determined with the PPC-05 chamber compared to the reference dose distribution leading to a significant displacement perturbation. If the ionization chamber is placed with P_{eff}, the dependence of p_Q on depth is much less pronounced with deviations of less than 7% over the complete range. When p_Q behind the Bragg peak at a depth of 265 mm is excluded, the variation is below 4%. As expected, the displacement perturbations are significantly smaller if the ionization chamber is positioned with P_{eff}. It needs to be noted that this definition of P_{eff} only corrects for the WET of the entrance window. For primary electron beams, the depth dependence of overall perturbations and the positioning is affected by further fluence perturbations Zink and Wulff (2009). Given the low range of secondary electrons in primary proton beams, these effects are expected to be of less relevance. Another explanation could be that, in the region of the Bragg peak, the stopping power ratios are not constant leading to a larger variability of WET and, hence, to changes in the shift between P_{eff} and P_{ref} resulting in substantial differences due to the local dose gradient. Nevertheless, more investigations would be required to fully understand the perturbations in the Bragg-peak region.

3.5. Impact of simplified field configurations in Monte Carlo simulations

Using an energy spread of 0.3% and 1% leads to differences of f_Q between P_{ref} and P_{eff} of 1.16% and 1.17%, respectively, which are similar to the difference of 1.19% found with the monoenergetic proton beam. For an energy spread of 10% as an upwards estimation, the effect of P_{eff} on the calculation of f_Q is with 1.22% slightly larger compared to the monoenergetic proton beam.

For scanned fields, different distances of the scanning magnets to the iso-center were investigated. For a large distance of 7 m, the effect of P_{eff} on f_Q is 1.18% whereas for a distance of 1 m (employing stronger trajectories of up to 2.9°) the effect is 1.09% which is slightly smaller compared to the result found with a perfectly parallel beam.

In conclusion, the simplified beam settings used in the Monte Carlo simulations are sufficiently accurate to investigate the effect of P_{eff} on the calculation of f_Q factors in clinical proton beams.

3.6. Analysis of best estimate of k_Q factors

Palmans *et al* (2022) derived best estimates of k_Q factors with average $\langle p_Q \rangle$ factors from published data. The authors made the assumption that the displacement correction factor p_{dis} is equal to unity for plane-parallel ionization chambers. However, all Monte Carlo derived data used P_{ref} for positioning. TRS-398 CoP, Rev. 1 defines P_{eff} for the positioning. The original analysis was repeated considering the displacement perturbation based on the dose gradient to correct the Monte Carlo based studies. In figure 4 part A), the analysis for the PPC-05 ionization chamber as done by Palmans *et al* (2022) is shown, calculating p_Q from published data without accounting for a displacement correction factor. In part B), the same analysis is shown however accounting for a displacement correction at the reference depth.

The effect for large residual ranges is negligible due to a small dose gradient. However, for small residual ranges the displacement correction leads to p_Q/p_{dis} being more constant over the complete range of residual ranges especially decreasing the scattering at low energies. The average ratio $\langle p_Q/p_{\text{dis}} \rangle$ is ∼0.5% larger than

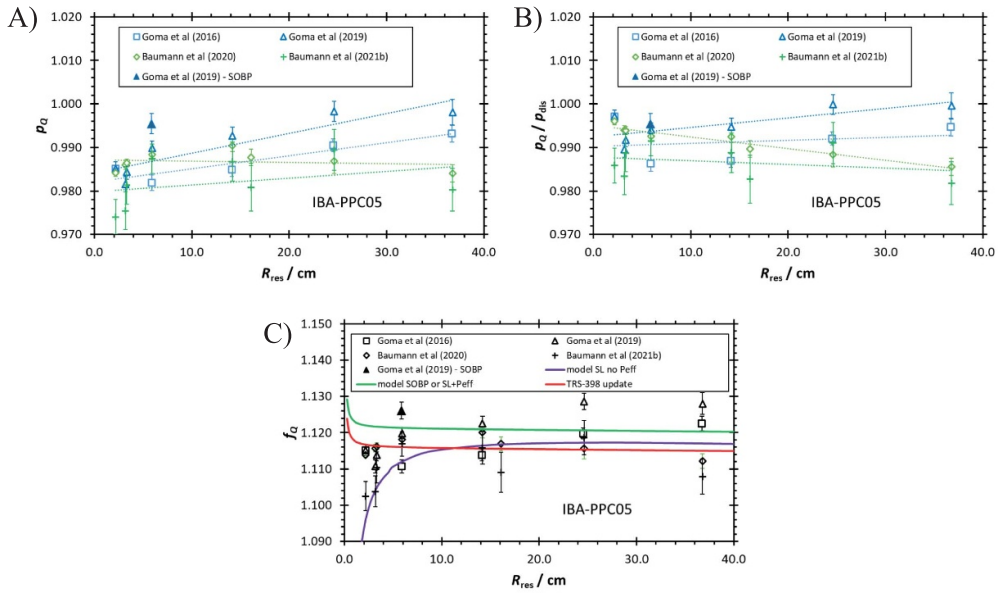

Figure 4. Average $\langle p_Q \rangle$ for the PPC-05 ionization chamber as a function of energy without (A) and with (B) accounting for displacement perturbations alongside with Monte Carlo calculated data published in the literature. In part (C) the best estimate of f_Q factors as a function of residual range for the original analysis done by Palmans *et al* (2022) in red, the new analysis from this study in green and the approach that ionization chambers are not positioned with P_{eff} but their P_{ref} at the measurement depth in purple. SL: single layer.

the average $\langle p_Q \rangle$. As a result, the best estimate of f_Q factors for the PPC-05 ionization chamber is also ~0.5% larger compared to the original analysis when accounting for the displacement correction as shown in part C). The line in red corresponds to the original analysis performed by Palmans *et al* (2022) and hence the values of f_Q used for the current TRS-398 CoP, Rev. 1. The green line corresponds to the same analysis, however, now accounting for the displacement effect, e.g. positioning of the ionization chamber with P_{eff} at the measurement depth. In this case, f_Q can be derived by multiplying $\langle p_Q/p_{dis} \rangle$ by $s_{w,air}$. The difference of 0.5% between the original analysis and the one from this study for the PPC-05 ionization chamber marks the worst case since the PPC-05 ionization chambers shows the largest shift between P_{ref} and P_{eff}. For all other ionization chambers, this effect is smaller. Furthermore, this difference is well inside the overall uncertainty of k_Q factors of 1.4%. Note that Palmans *et al* (2022) used an approach so that these factors can be used both for single energy layers (SL) and spread-out Bragg peaks (SOBP).

Additionally shown in part C) is the corresponding f_Q factor if the ionization chamber is not positioned with P_{eff} at the measurement depth but with P_{ref}. This case impacts only single energy layers (SL) since the dose gradient within an SOBP is negligible. In this case, f_Q can be derived by multiplying $\langle p_Q/p_{dis} \rangle$ not only by $s_{w,air}$ but also by p_{dis}, e.g. $f_Q = \langle p_Q/p_{dis} \rangle \cdot p_{dis} \cdot s_{w,air}$. As can be seen, p_{dis} has the largest effect for small residual ranges leading to significant changes in f_Q. So, positioning the ionization chamber without accounting for P_{eff} combined with using the data from TRS-398 CoP, Rev. 1, would result in smaller errors at high energies, but substantial errors at low energies and we therefore tend to advice against this option.

4. Conclusion

The effect of positioning plane-parallel ionization chambers at the measurement depth on the calculation of f_Q and hence k_Q factors was investigated in this study with the help of Monte Carlo simulations. It was shown that f_Q and thus k_Q varies by up to 1.2% when ionization chambers are positioned with P_{eff} instead of with P_{ref}. This change is mainly caused by the gradient of the absorbed dose-to-water at the measurement depth.

In general, the difference of f_Q between positioning the ionization chamber with P_{ref} compared to P_{eff} is larger for 1) larger dose gradients (or lower proton energies) and 2) larger shifts between P_{ref} and P_{eff}.

The impact on k_Q factors published in the updated version of TRS-398 CoP is small with 0.5% at maximum for the PPC-05 ionization chamber. Therefore, we tend to recommend positioning the ionization chamber accounting for P_{eff} and using the data from TRS-398 CoP, Rev. 1.

Data availability statement

The data cannot be made publicly available upon publication because no suitable repository exists for hosting data in this field of study. The data that support the findings of this study are available upon reasonable request from the authors.

Acknowledgments

The Project was partially supported by the Federal Ministry of Education and Research within the scope of the Grant 'Biological and physical optimization of particle beams: radiation protection for the patient' (PARTITUR, Grant number 02NUK076A). This study was partially funded by the Hessen State Ministry of Higher Education, Research, and the Arts (HMWK) via the LOEWE Research Cluster "ADMIT", grant LOEWE/2/16/519/03/09.001(0001)/101.

ORCID iDs

Kilian-Simon Baumann https://orcid.org/0000-0003-1223-523X
Jörg Wulff https://orcid.org/0000-0001-8260-3523
Gloria Vilches-Freixas https://orcid.org/0009-0009-5478-9389
Hugo Palmans https://orcid.org/0000-0002-0235-5118

References

2024 Private communication with Stanislav Vatnitsky, n.d..
AEA 2000 *Technical Reports Series* (International Atomic Energy Agency) (available at: www.iaea.org/publications/5954/absorbed-dose-determination-in-external-beam-radiotherapy)
Agostinelli S *et al* 2003 Geant4 - a simulation toolkit *Nucl. Instrum. Methods Phys. Res.* A **506** 250–303
Andreo P, Wulff J, Burns D T and Palmans H 2013 Consistency in reference radiotherapy dosimetry: resolution of an apparent conundrum when 60co is the reference quality for charged-particle and photon beams *Phys. Med. Biol.* **58** 6593–621
Baumann K-S, Derksen L, Witt M, Adeberg S and Zink K 2023 The influence of different versions of fluka and geant4 on the calculation of response functions of ionization chambers in clinical proton beams *Phys. Med. Biol.* **68** 24NT01
Baumann K-S, Derksen L, Witt M, Burg J M, Engenhart-Cabillic R and Zink K 2021 Monte carlo calculation of beam quality correction factors in proton beams using fluka *Phys. Med. Biol.* **66** 17NT01
Baumann K-S, Gomà C, Wullf J, Kretschmer J and Zink K 2023 Monte carlo calculated ionization chamber correction factors in clinical proton beams – deriving uncertainties from published data *Phys. Medica* **113** 102655
Baumann K-S, Kaupa S, Bach C, Engenhart-Cabillic R, Zink K 2020a Monte carlo calculation of beam quality correction factors in proton beams using TOPAS/GEANT4 *Phys. Med. Biol.* **65** 055015
Baumann K-S, Kaupa S, Bach C, Engenhart-Cabillic R and Zink K 2020 Monte carlo calculation of perturbation correction factors for air-filled ionization chambers in clinical proton beams using TOPAS/GEANT4 *Z. Med. Phys.* **31** 175–91
Bielajew A F 2016 *Fundamentals of the Monte Carlo method for neutral and charged particle transport* (The University of Michigan Department of Nuclear Engineering and Radiological Sciences)
Gomà C, Andreo P and Sempau J 2016 Monte carlo calculation of beam quality correction factors in proton beams using detailed simulation of ionization chambers *Phys. Med. Biol.* **61** 2389–406
Gomá C and Sterpin E 2019 Monte carlo calculation of beam quality correction factors in proton beams using penh (accepted manuscript) *Phys. Med. Biol.* **64** 185009
IAEA 2024 *Technical Reports Series* (International Atomic Energy Agency) (available at: www.iaea.org/publications/15048/absorbed-dose-determination-in-external-beam-radiotherapy)
Kretschmer J, Dulkys A, Brodbek L, Stelljes T S, Looe H K and Poppe B 2020 Monte carlo simulated beam quality and perturbation correction factors for ionization chambers in monoenergetic proton beams *Med. Phys.* **47** 5890–905
Lourenço A, Wellock N, Thomas R, Homer M, Bouchard H, Kanai T, MacDougall N, Royle G and Palmans H 2016 Theoretical and experimental characterization of novel water-equivalent plastics in clinical high-energy carbon-ion beams *Phys. Med. Biol.* **61** 7623
Palmans H, Lourenędiio A, Medin J, Vatnitsky S Andreo P 2022 Current best estimates of beam quality correction factors for reference dosimetry of clinical proton beams *Phys. Med. Biol.* **67** 195012
Palmans H, Medin J, Trnková P and Vatnitsky S 2020 Gradient corrections for reference dosimetry using farmer-type ionization chambers in single-layer scanned proton fields *Med. Phys.* **47** 6531–9
Perl J, Shin J, Schuemann J, Faddegon B and Paganetti H 2012 Topas: an innovative proton Monte Carlo platform for research and clinical applications *Med. Phys.* **39** 6818–37
RTNORM 2019 Radiotherapy normative, ionizing radiation dosimetry for radiotherapy, euramet/empir research project (available at: www.rtnorm.eu) (Accessed 23 June 2024)
Seltzer S M, Fernández-Verea J M, Andreo P, Bergstrom P M, Burns D T, Krajcar Bronić I, Ross C K and Salvat F 2016 Key data for ionizing-radiation dosimetry: measurement standards and applications. icru report 90 *J. ICRU* **14** 1–110
Sempau J, Andreo P, Aldana J, Mazurier J and Salvat F 2004 Electron beam quality correction factors for plane-parallel ionization chambers: Monte Carlo calculations using the PENELOPE system *Phys. Med. Biol.* **49** 4427–44
Vilches-Freixas G, Bosmans G, Douralis A, Martens J, Meijers A, Rinaldi I, Salvo K, Thomas R, Palmans H and Lourenço A 2024 Experimental comparison of cylindrical and plane parallel ionization chambers for reference dosimetry in continuous and pulsed scanned proton beams *Phys. Med. Biol.* **69** 105021
Vilches-Freixas G, Unipan M, Rinaldi I, Martens J, Roijen E, Almeida I P, Decabooter E and Bosmans G 2020 Beam commissioning of the first compact proton therapy system with spot scanning and dynamic field collimation *Br. J. Radiol.* **93** 20190598

Wulff J, Baumann K-S, Verbeek N, Bäumer C, Timmermann B and Zink K 2018 TOPAS/geant4 configuration for ionization chamber calculations in proton beams *Phys. Med. Biol.* **63** 115013

Zhang R Newhauser W D 2009 Calculation of water equivalent thickness of materials of arbitrary density, elemental composition and thickness in proton beam irradiation *Phys. Biol.* **54** 1383

Zhang R, Taddei P J, Fitzek M M and Newhauser W D 2010 Water equivalent thickness values of materials used in beams of protons, helium, carbon and iron ions *Phys. Biol.* **55** 2481

Zink K, Baumann K-S, Theiss U, Subtil F, Lahrmann S, Eberle F and Adeberg S 2024 Organization and operation of multi particle therapy facilities: the Marburg Ion-Beam Therapy Center, Germany (MIT) *Health Technol.* **14** 929–38

Zink K and Wulff J 2009 Positioning of a plane-parallel ionization chamber in clinical electron beams and the impact on perturbation factors *Phys. Med. Biol.* **54** 2421